Viscosities of the Gay-Berne Nematic Liquid Crystal

A. M. Smondyrev,[1] George B. Loriot,[2] and Robert A. Pelcovits[1]
[1]*Department of Physics, Brown University, Providence, Rhode Island 02912*
[2]*Computing and Information Services, Brown University, Providence, Rhode Island 02912*
(Received 3 May 1995)

We present molecular dynamics simulation measurements of the viscosities of the Gay-Berne phenomenological model of liquid crystals in the nematic and isotropic phases. The temperature dependence of the rotational and shear viscosities, including the nonmonotonic behavior of one shear viscosity, are in good agreement with experimental data. The bulk viscosities are significantly larger than the shear viscosities, again in agreement with experiment.

PACS numbers: 61.30.Cz, 64.70.Md

Ever increasing computer power has made simulations of simple, yet realistic, molecular models of liquid crystals a feasible enterprise. With the aid of computers it is possible to study the effects of molecular shapes, sizes, and interactions on macroscopic behavior. Three types of liquid crystal models have been used in simulation work. The first is the Lebwohl-Lasher model [1], a lattice model for rotators. This model can be used to study the isotropic-nematic transition as a rotational order-disorder transition in an effective crystalline solid. Another class of models which has received much attention and includes the translational degrees of freedom of a liquid crystal uses hard particles of various shapes that interact solely by excluded volume effects [2,3]. These hard body models exhibit very rich phase diagrams including smectic, columnar, and cubatic phases. Finally, in recent years there has been considerable numerical study of the Gay-Berne (GB) system [4], which is a fluid of pointlike particles, each carrying a unit vector $\hat{\mathbf{u}}$ that mimics the long molecular axis. The particles interact via an anisotropic Lennard-Jones potential, which depends on the relative orientation and location of a pair of molecules. This system displays rich behavior like the hard body models, but also includes attractive forces. These latter forces play an especially important role in the formation of smectic phases, which are more readily formed in the GB system than in the hard body models. The GB model has also been extended to include chirality [5] and to model discotics [6]. Unlike the hard body models the GB system can also exhibit thermotropic transitions.

Previous studies of the GB system have focused on the phase diagram [7–9], single-particle translational and rotational dynamics [10], and heat flow [11]. In this Letter we report on numerical measurements of the viscosities of the GB system as a function of temperature (other authors have measured the viscosities for a purely repulsive GB potential at a single temperature [12]). We find a number of results which indicate that the GB model exhibits the principal dynamical features of a real nematic liquid crystal. The temperature dependence of the shear viscosities and the rotational viscosity below the isotropic-nematic transition is qualitatively similar to what is observed in experiment [13–16], including the nonmonotonic behavior of one of the shear viscosities. The two bulk viscosities are an order of magnitude larger than the shear viscosities in agreement with ultrasonic measurements [17]. We also find that long-time correlations of the director exhibit the expected Brownian motion due primarily to the finite size of our system.

The GB potential is modeled to give the best fit to the pair potential for a molecule consisting of a linear array of four equidistant Lennard-Jones centers with a separation of $2\sigma_0$ between the first and fourth sites (subsequent work [9] examined different fits). The GB potential is given by

$$U(\hat{\mathbf{u}}_1,\hat{\mathbf{u}}_2,\mathbf{r}) = 4\varepsilon(\hat{\mathbf{u}}_1,\hat{\mathbf{u}}_2,\mathbf{r})\left[\left\{\frac{\sigma_0}{r-\sigma(\hat{\mathbf{u}}_1,\hat{\mathbf{u}}_2,\mathbf{r})+\sigma_0}\right\}^{12} - \left\{\frac{\sigma_0}{r-\sigma(\hat{\mathbf{u}}_1,\hat{\mathbf{u}}_2,\mathbf{r})+\sigma_0}\right\}^{6}\right], \tag{1}$$

where $\hat{\mathbf{u}}_1,\hat{\mathbf{u}}_2$ are unit vectors giving the orientations of the two molecules separated by the position vector $\mathbf{r}$. The parameters $\varepsilon(\hat{\mathbf{u}}_1,\hat{\mathbf{u}}_2,\mathbf{r})$ and $\sigma(\hat{\mathbf{u}}_1,\hat{\mathbf{u}}_2,\mathbf{r})$ are orientation dependent and give the well depth and intermolecular separation where $U = 0$, respectively. The well depth is written as

$$\varepsilon(\hat{\mathbf{u}}_1,\hat{\mathbf{u}}_2,\mathbf{r}) = \varepsilon_0\varepsilon^{\nu}(\hat{\mathbf{u}}_1,\hat{\mathbf{u}}_2)\varepsilon'^{\mu}(\hat{\mathbf{u}}_1,\hat{\mathbf{u}}_2,\mathbf{r}), \tag{2}$$

where

$$\varepsilon(\hat{\mathbf{u}}_1,\hat{\mathbf{u}}_2) = [1-\chi^2(\hat{\mathbf{u}}_1\cdot\hat{\mathbf{u}}_2)^2]^{-1/2} \tag{3}$$

and

$$\varepsilon'(\hat{\mathbf{u}}_1,\hat{\mathbf{u}}_2,\hat{\mathbf{r}}) = 1 - \frac{\chi'}{2}\left\{\frac{(\hat{\mathbf{r}}\cdot\mathbf{u}_1+\hat{\mathbf{r}}\cdot\mathbf{u}_2)^2}{1+\chi'(\mathbf{u}_1\cdot\mathbf{u}_2)} + \frac{(\hat{\mathbf{r}}\cdot\mathbf{u}_1-\hat{\mathbf{r}}\cdot\mathbf{u}_2)^2}{1-\chi'(\mathbf{u}_1\cdot\mathbf{u}_2)}\right\}. \tag{4}$$

The shape anisotropy parameter χ is given by

$$\chi = \{(\sigma_e/\sigma_s)^2 - 1\}/\{(\sigma_e/\sigma_s)^2 + 1\}, \tag{5}$$

where σ_e and σ_s are the separation of end-to-end and side-by-side molecules, respectively. The parameter χ' is

 0031-9007/95/75(12)/2340(4)$06.00

given by

$$\chi' = \{1 - (\varepsilon_e/\varepsilon_s)^{1/\mu}\}/\{1 + (\varepsilon_e/\varepsilon_s)^{1/\mu}\}. \quad (6)$$

The ratio of the well depths for end-to-end and side-by-side configurations is $\varepsilon_e/\varepsilon_s$.

We simulated a system of $N = 256$ particles using the molecular dynamics technique. The ratio σ_e/σ_s was set equal to 3, the ratio $\varepsilon_e/\varepsilon_s = 5$, and exponents $\nu = 1$ and $\mu = 2$. These values yield the best fit to the linear array of four Lennard-Jones centers [4], though other values have been used [8,9]. The moment of inertia was chosen to be $4m\sigma_0^2$, as in Ref. [8]. We used cubic periodic boundary conditions, and cut off and smoothed the potential at $3.8\sigma_0$. The equations of motion were solved using the leap-frog algorithm with integration time step $\Delta t^* = 0.001$ in reduced units [$\Delta t^* = \Delta t(m\sigma_0^2/\varepsilon_0)^{-1/2}$, where m is the mass of the molecule]. Translational and rotational temperatures were controlled using the Nose-Hoover thermostat [18]. The initial configuration was generated by locating nearly parallel GB molecules on the sites of an fcc lattice at low scaled density, $\rho^*(\equiv N\sigma_0^3/V) = 0.10$. We carried out a long run (20 000 iterations), which reduced the nematic order parameter to a value of 0.12, and disordered the system translationally. The system was then gradually compressed at constant scaled temperature $T^*(\equiv k_BT/\varepsilon_0) = 3.0$ to a density $\rho^* = 0.32$. Finally, at constant density the temperature was lowered in small steps to the isotropic-nematic transition temperature and below. At this stage longer simulation runs (180 000–300 000 iterations) were performed to obtain the values of the viscosities.

The dynamical description of a compressible nematic requires six viscosities: three shear viscosities, ν_1, ν_2, and ν_3; two bulk viscosities, $\nu_4 - \nu_2$ and ν_5; and a director rotational viscosity, γ_1. To calculate these viscosities from correlation functions of the stress tensor and the director, we transformed to a coordinate system where the 3 axis is parallel to the average orientation of the director, and the 1 and 2 axes are perpendicular to the director. The elements of the stress tensor are defined by

$$\sigma_{\alpha\beta} = \frac{1}{V}\left(\sum_i p_\alpha^i p_\beta^j/m + \sum_i \sum_{j>i} r_\alpha^{ij} f_\beta^{ij}\right), \quad \alpha, \beta = 1, 2, 3, \quad (7)$$

where V is the volume of the system, $\mathbf{p}^i$ is the linear momentum of molecule i, and $\mathbf{r}^{ij}$ and $\mathbf{f}_{ij}$ are, respectively, the relative position vector and force between molecules i and j. The five viscosities ν_1, ν_2, ν_3, ν_4, and ν_5 associated with shear and compression are then given in terms of Kubo-like formulas [19],

$$\nu_1 = \frac{V}{2k_BT}\int_0^\infty dt\{\langle[\sigma_{33}(t) - \sigma(t)][\sigma_{33}(0) - \sigma(0)]\rangle - \langle\sigma_{12}(t)\sigma_{12}(0)\rangle\}, \quad (8)$$

$$\nu_2 = \frac{V}{k_BT}\int_0^\infty dt\,\langle\sigma_{12}(t)\sigma_{12}(0)\rangle, \quad (9)$$

$$\nu_3 = \frac{V}{k_BT}\int_0^\infty dt\,\langle\sigma_{13}(t)\sigma_{13}(0)\rangle, \quad (10)$$

$$\nu_4 = \frac{V}{k_BT}\int_0^\infty dt\,\langle\sigma(t)\sigma(0)\rangle, \quad (11)$$

$$\nu_5 = \frac{V}{k_BT}\int_0^\infty dt\,\langle\sigma_{33}(t)\sigma(0)\rangle, \quad (12)$$

where

$$\sigma(t) = \tfrac{1}{2}[\sigma_{11}(t) + \sigma_{22}(t)]. \quad (13)$$

The time-correlation functions appearing in Eqs. (8)–(12) were evaluated by averaging over successive time origins [20]. The components of the stress tensor were evaluated first in the cubic coordinate system (with axes parallel to the sides of the cell) where we defined periodic boundary conditions and then transformed to the director coordinate frame.

In order to compare our simulation results with experimental measurements of shear viscosities, we applied a magnetic field H along the direction of nematic ordering, with $\chi_a H^2 = 1.0$ in our reduced units (χ_a is the anisotropy in the magnetic susceptibility). Experiments typically measure Miesowicz viscosities [13],

$$\eta_1 = \nu_3 + \tfrac{1}{4}\gamma_1(1 - \lambda)^2 + \lambda\gamma_1, \quad (14)$$

$$\eta_2 = \nu_3 + \tfrac{1}{4}\gamma_1(1 - \lambda)^2, \quad (15)$$

$$\eta_3 = \nu_2. \quad (16)$$

The parameter λ is a reactive coefficient [19] that determines the response of the director to shear flow. Because we have not yet performed a direct shear flow experiment we do not have a value of λ for the GB system; in *p*-azoxyanisole (PAA) [19] $\lambda = 1.15 \pm 0.10$. We have assumed that λ is unity in the GB system and computed Miesowicz viscosities from our measurements; a 10% change in this value of λ will not alter the qualitative features of our results. Results for the three Miesowicz shear viscosities are shown in Figs. 1 and 2; results for γ_1 alone are given in Fig. 3. The large value of H needed to stabilize the director motion smears the nematic-isotropic transition. At sufficiently high temperatures where the nematic order parameter is low (see the inset of Fig. 1) the system is essentially isotropic with large director fluctuations, and we have plotted the average of the two shear viscosities η_2 and η_3 as a single isotropic viscosity. Below the temperature $T \simeq 2.0$ where the nematic order parameter becomes substantial we note that η_2 decreases at first as the temperature is lowered and then rises. This effect has been observed experimentally in PAA [13,14], *N*-(4′-methoxybenzilidene)-4-(*n*-butyl)aniline (MBBA) [14], and in the cyanobiphenyl homologs [16]. The viscosity η_2 is associated with shear flow parallel to the director, so its value drops when the nematic order becomes appreciable. Its subsequent rise is not fully understood. Likewise the fact that $\eta_3 > \eta_2$ below the transition has also been observed [13,14], and deep in the nematic phase the

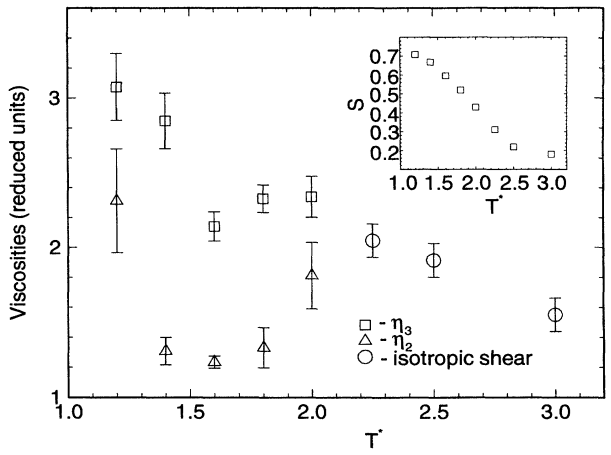

FIG. 1. The isotropic shear and two of the Miesowicz viscosities in reduced units as functions of the scaled temperature T^*, in the presence of a magnetic field. The inset shows the nematic order parameter S as a function of T^* for the same value of magnetic field.

ratio η_3/η_2 has been found to be approximately 1.5, in both PAA and MBBA, in good agreement with our results. The temperature dependence of ν_1 or η_1 has not been measured, but the value of ν_1 deep in the nematic phase of PAA is known [17] and is comparable to the value of η_3. We find $\nu_1 = 2.25$ and 1.55 (reduced units) at $T^* = 1.2$ and 1.4, respectively. We have also measured the bulk viscosities at these latter temperatures and find $\nu_4 = 29.0$ and 14.1; $\nu_5 = 38.33$ and 15.9 (reduced units), respectively. Experimental measurements of the bulk viscosities deep in the nematic phase of PAA and para-azoxyphenetole (PAP) [17] also show values that are an order of magnitude larger than the largest shear viscosity. The temperature dependence of the bulk viscosities has not been explored experimentally. Numerically determining the bulk viscosities is more time consuming than determining the shear viscosities, so we have not explored their full temperature dependence.

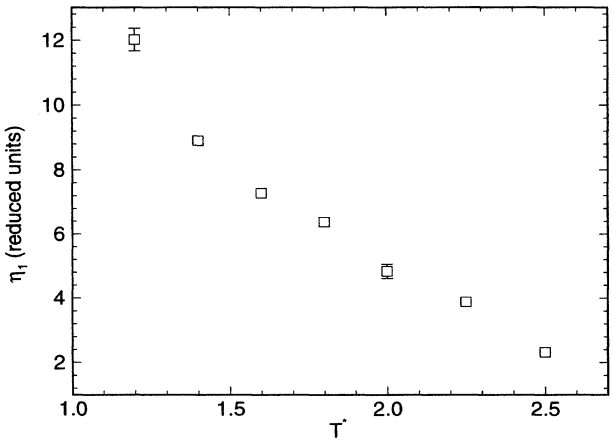

FIG. 2. The third Miesowicz viscosity, η_1, which is 2 to 3 times larger than the other two viscosities; compare Fig. 1.

Correlations in the director rotational motion and the value of the rotational viscosity γ_1 are best studied by measuring the correlation function:

$$C(t) = \langle [\delta n(t) - \delta n(0)]^2 \rangle, \tag{17}$$

where

$$\delta n(t) = \tfrac{1}{2}[n_1(t) + n_2(t)]. \tag{18}$$

The director components n_1 and n_2 are the eigenvectors of the order parameter tensor,

$$Q_{\alpha\beta} = \frac{1}{N}\sum_i \left(\frac{3u_{i\alpha}u_{i\beta} - \delta_{\alpha\beta}}{2}\right), \qquad \alpha = 1,2,3, \tag{19}$$

corresponding to the two lowest eigenvalues.

If the director motion is diffusive (Brownian motion), then $C(t)$ at long times will follow:

$$C(t) \sim 2\gamma_1^{-1} t, \tag{20}$$

and the value of γ_1 can be extracted with excellent statistics [21]. This behavior was observed in our system (see Fig. 4) at sufficiently long times, and is sensible given the magnetic field and especially the small system size. At shorter times the director motion obeys the form $C(t) \sim t^2$ approximately, which is to be expected for ballistic behavior. For much larger system sizes and small magnetic fields we would expect this latter behavior to persist to larger times due to the presence of massless Goldstone modes [22], even though the microscopic director motion is no longer ballistic. This Goldstone-like behavior has been reported by Zhang *et al.* [23], in Monte Carlo studies of the Lebwohl-Lasher lattice model where very large system sizes are readily studied. The temperature dependence of γ_1 is given in Fig. 3 in the form of an Arrhenius plot, i.e., $\gamma_1 \propto \exp(E/k_BT)$, where E is an activation energy. We have also attempted to fit our data to the form $\gamma_1 \propto S\exp(E/k_BT)$, where S is the nematic order parameter; this form fits experimental

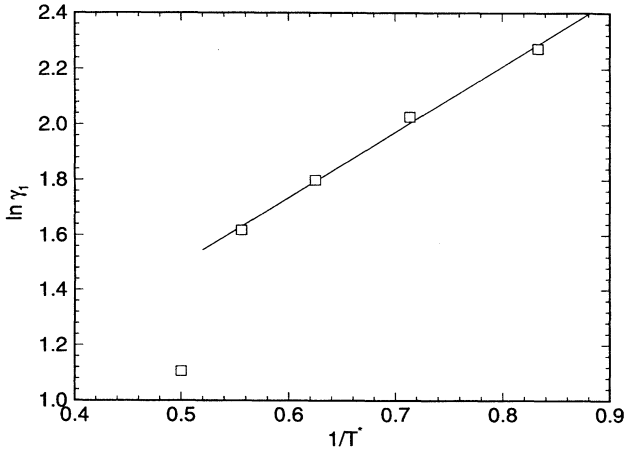

FIG. 3. The rotational viscosity γ_1 in reduced units as a function of scaled temperature indicating the activated form of the dependence.

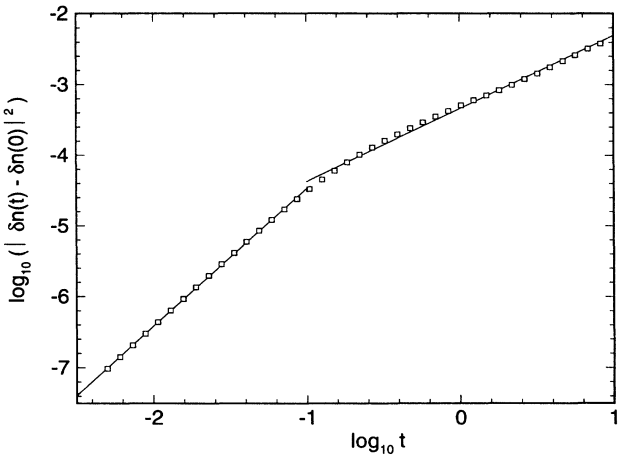

FIG. 4. The director correlation function $C(t)$, Eq. (17), as a function of dimensionless time, at $T^* = 1.4$. The short-time behavior is fit by a straight line with slope 1.92, while the slope at long times is 1.00. The error bars are imperceptible on this scale.

data [24,25] very well. However, our limited number of data points are fit almost equally well with or without the factor of S, so we cannot state definitively which form is more accurate.

We are grateful to Professor Seth Fraden for helpful suggestions. A. M. S. and R. A. P. were supported in part by the National Science Foundation under Grant No. DMR92-17290.

[1] P. A. Lebwohl and G. Lasher, Phys. Rev. A **6**, 426 (1972).
[2] D. Frenkel, in *Phase Transitions in Liquid Crystals,* edited by S. Martellucci and A. N. Chester (Plenum, New York, 1992).
[3] M. P. Allen, Philos. Trans. R. Soc. London A **344**, 323 (1993).
[4] J. G. Gay and B. J. Berne, J. Chem. Phys. **74**, 3316 (1981).
[5] A. L. Tsykalo, Mol. Cryst. Liq. Cryst. **129**, 409 (1985).
[6] A. P. J. Emerson, G. R. Luckhurst, and S. G. Whatling, Mol. Phys. **82**, 113 (1994).
[7] E. DeMiguel, L. F. Rull, M. K. Chalam, and K. E. Gubbins, Mol. Phys. **74**, 405 (1991).
[8] G. R. Luckhurst, R. A. Stephens, and R. W. Phippen, Liq. Cryst. **8**, 451 (1990).
[9] G. R. Luckhurst and P. S. J. Simmonds, Mol. Phys. **80**, 233 (1993).
[10] E. DeMiguel, L. F. Rull, and K. E. Gubbins, Phys. Rev. A **45**, 3813 (1992).
[11] S. Sarman and D. J. Evans, J. Chem. Phys. **99**, 620 (1993); S. Sarman, J. Chem. Phys. **101**, 480 (1994).
[12] S. Sarman and D. J. Evans, J. Chem. Phys. **99**, 9021 (1993).
[13] M. Miesowicz, Nature (London) **158**, 27 (1946).
[14] D. Langevin, J. Phys. (Paris) **33**, 249 (1972).
[15] See, e.g., W. H. de Jeu, *Physical Properties of Liquid Crystalline Materials* (Gordon and Breach, New York, 1980).
[16] A. G. Chmielewski, Mol. Cryst. Liq. Cryst. **132**, 339 (1986).
[17] K. A. Kemp and S. V. Letcher, Phys. Rev. Lett. **27**, 1634 (1971).
[18] S. Nose, Mol. Phys. **52**, 255 (1984); W. G. Hoover, Phys. Rev. A **31**, 1695 (1985).
[19] D. Forster, Ann. Phys. (N.Y.) **84**, 505 (1974).
[20] M. P. Allen and D. J. Tildesley, *Computer Simulation of Liquids* (Oxford University Press, Oxford, 1987).
[21] It is also possible to measure γ_1 from a time correlation function of $\dot{n}_\alpha$, the time derivative of the director. We have done so and obtained essentially identical results.
[22] C. Yeung, M. Rao, and R. Desai, Phys. Rev. Lett. **73**, 1813 (1994).
[23] Z. Zhang, O. G. Mouritsen, K. Otnes, T. Riste, and M. J. Zuckermann, Phys. Rev. Lett. **70**, 1834 (1993).
[24] J. Prost, G. Sigaud, and B. Regaya, J. Phys. (Paris), Lett. **37**, L341 (1976).
[25] W. H. de Jeu, Phys. Lett. A **69**, 122 (1978).